Multilevel Approach for Simulating the Reorientation of Mesogens in Nematic Liquid Crystal Elastomers

Francesca Concas and Michael Groß

Professorship of Applied Mechanics and Dynamics
Department of Mechanical Engineering
Technische Universität Chemnitz

ACEX2025 - Naples, Italy

30 June - 4 July 2025

TECHNISCHE UNIVERSITÄT CHEMNITZ

DFG Deutsche Forschungsgemeinschaft

Acknowledgments: This research is provided by DFG grant GR 3297/7-1.

Motivation and goals

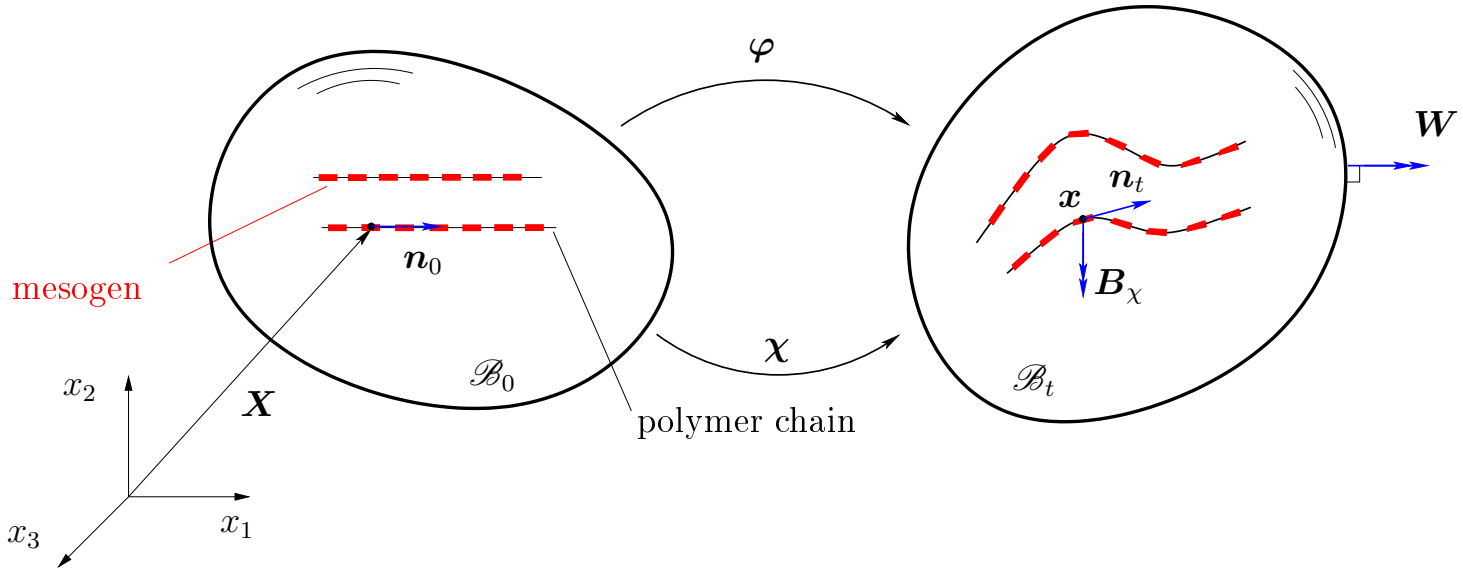

[Concas and Groß (2023)]

Motivation

- nematic liquid crystal elastomers (LCEs) are innovative materials showing unique responses to external stimuli, e.g. electric fields
- possible applications: soft robotics, artificial muscles, etc.
- simulations of nematic LCEs can be computationally very expensive by using mixed finite elements
  - large number of elements to detect microstructural phenomena such as arise of stripe domains
  - large number of fields for predicting their unique behaviour
- our previous approach (see Concas and Groß (2023),(2024),(2025) based on the computation for each time step of **all** fields by the **global** tangent including all nodes of the whole virtual specimen, i.e. **global-level procedure**) can be improved in order to reduce the amount of global degrees of freedom

Goals

- implement a **multi-level procedure** (similar to the **Multilevel-Newton method** of Ellsiepen and Hartmann (2001)) $\rightarrow$ identify **global** and **local fields**
  - **static condensation** for including local variables into the global tangent
  - global and local residuals have to fulfill different convergence criteria $\rightarrow \|\boldsymbol{R}_G\|_\infty < TOL_G$ and $\|\boldsymbol{R}_L\|_\infty < TOL_L$ with $TOL_L = 10^{-2} TOL_G$
- define a rotational free energy density $\psi\,(\boldsymbol{\alpha},\, \boldsymbol{\beta})$ so that the **local tangent** is not singular
- define Dirichlet boundary conditions for the orientational mapping $\boldsymbol{\chi}$ associated to the mesogens, i.e. nematic director $\boldsymbol{n}_t$
- compare results obtained by the **multi-level procedure**, in which a full rotation of the nematic director is achieved, with results from the **global-level procedure**

Diagram of the multi-level procedure

cf. Felippa and Park (1979)

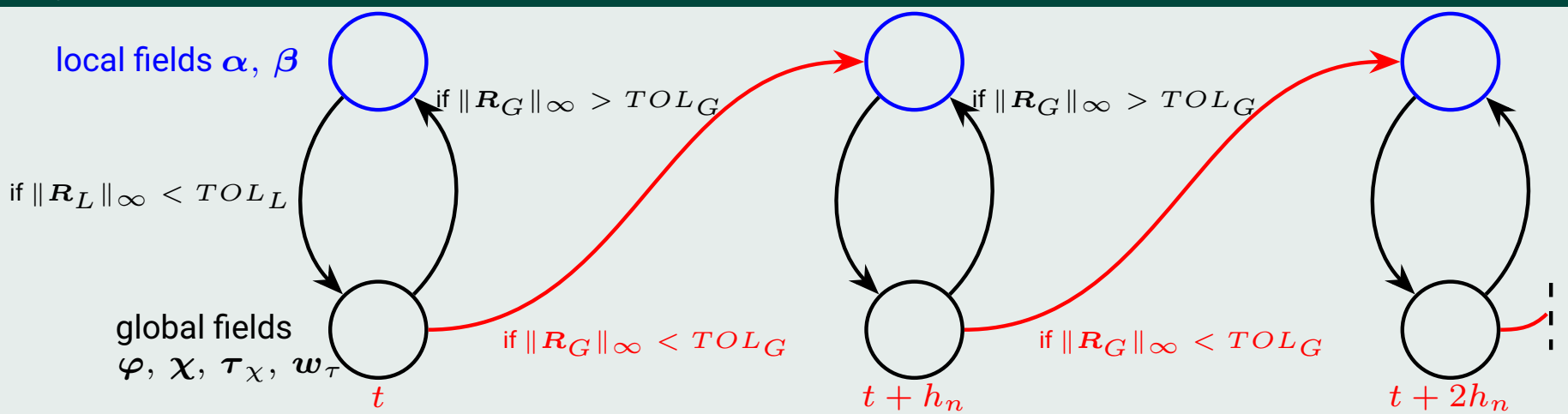

Global and local fields

cf. principle of virtual power from Concas and Groß (2023), (2024)

- **global fields**
  - $\boldsymbol{\varphi}$ deformation mapping of the position $\boldsymbol{x}$ between the initial configuration $\mathscr{B}_0$ and the current configuration $\mathscr{B}_t$
  - $\boldsymbol{\chi}$ orientation mapping of the nematic director $\boldsymbol{n}_t$ (direction of mesogens in a monodomain specimen) between $\mathscr{B}_0$ and $\mathscr{B}_t$
  - $\boldsymbol{\tau}_\chi$ Lagrange multiplier for the constraint $\dot{\boldsymbol{\chi}} = \left(\dot{\boldsymbol{\alpha}} - \dot{\boldsymbol{\beta}}\right) \times \boldsymbol{\chi}$
  - $\boldsymbol{w}_\tau$ Lagrange multiplier for the constraint $\dot{\boldsymbol{\alpha}} = -\frac{1}{2}\boldsymbol{\epsilon} : \dot{\boldsymbol{F}}\boldsymbol{F}^{-1}$
- **local fields**
  - $\boldsymbol{\beta}$ rotation mapping of the mesogens between $\mathscr{B}_0$ and $\mathscr{B}_t$
  - $\boldsymbol{\alpha}$ rotation mapping of rotations occurring in the bulk elastomer between $\mathscr{B}_0$ and $\mathscr{B}_t$

System of equations

$$\boldsymbol{K}_{\varphi\varphi}\Delta\boldsymbol{\varphi} + \boldsymbol{K}_{\varphi\chi}\Delta\boldsymbol{\chi} + \boldsymbol{K}_{\varphi\alpha}\Delta\boldsymbol{\alpha} + \boldsymbol{K}_{\varphi w}\Delta\boldsymbol{w}_\tau + \boldsymbol{K}_{\varphi\beta}\Delta\boldsymbol{\beta} = \boldsymbol{R}_\varphi \quad (1)$$

$$\boldsymbol{K}_{\chi\varphi}\Delta\boldsymbol{\varphi} + \boldsymbol{K}_{\chi\chi}\Delta\boldsymbol{\chi} + \boldsymbol{K}_{\chi\alpha}\Delta\boldsymbol{\alpha} + \boldsymbol{K}_{\chi\tau}\Delta\boldsymbol{\tau}_\chi + \boldsymbol{K}_{\chi\beta}\Delta\boldsymbol{\beta} = \boldsymbol{R}_\chi \quad (2)$$

$$\boldsymbol{K}_{w\varphi}\Delta\boldsymbol{\varphi} + \boldsymbol{K}_{w\alpha}\Delta\boldsymbol{\alpha} = \boldsymbol{R}_w \quad (3)$$

$$\boldsymbol{K}_{\tau n}\Delta\boldsymbol{\chi} + \boldsymbol{K}_{\tau\alpha}\Delta\boldsymbol{\alpha} + \boldsymbol{K}_{\tau\beta}\Delta\boldsymbol{\beta} = \boldsymbol{R}_\tau \quad (4)$$

$$\boldsymbol{K}_{\alpha\varphi}\Delta\boldsymbol{\varphi} + \boldsymbol{K}_{\alpha\chi}\Delta\boldsymbol{\chi} + \boldsymbol{K}_{\alpha\alpha}\Delta\boldsymbol{\alpha} + \boldsymbol{K}_{\alpha w}\Delta\boldsymbol{w}_\tau + \boldsymbol{K}_{\alpha\tau}\Delta\boldsymbol{\tau}_\chi + \boldsymbol{K}_{\alpha\beta}\Delta\boldsymbol{\beta} = \boldsymbol{R}_\alpha \quad (5)$$

$$\boldsymbol{K}_{\beta\varphi}\Delta\boldsymbol{\varphi} + \boldsymbol{K}_{\beta\chi}\Delta\boldsymbol{\chi} + \boldsymbol{K}_{\beta\alpha}\Delta\boldsymbol{\alpha} + \boldsymbol{K}_{\beta\tau}\Delta\boldsymbol{\tau}_\chi + \boldsymbol{K}_{\beta\beta}\Delta\boldsymbol{\beta} = \boldsymbol{R}_\beta \quad (6)$$

Algorithm

for $i-th$ *time step* **do**

- ▶ calculate global residuals $\boldsymbol{R}_G = \left\{ \boldsymbol{R}_\varphi \ \boldsymbol{R}_\chi \ \boldsymbol{R}_\tau \ \boldsymbol{R}_w \right\}^T$
- **for** $j-th$ *global Newton loop* **do**
  - ▶ calculate local residuals $\boldsymbol{R}_L = \left\{ \boldsymbol{R}_\alpha \ \boldsymbol{R}_\beta \right\}^T$
  - **for** $k-th$ *Newton loop for* ***each*** *element (local Newton loop)* **do**
    - ▶ calculate tangents $\boldsymbol{K}_{\alpha\alpha}, \boldsymbol{K}_{\alpha\beta}, \boldsymbol{K}_{\beta\alpha}$ and $\boldsymbol{K}_{\beta\beta}$
    - ▶ solve system of equations $\begin{bmatrix} \boldsymbol{K}_{\alpha\alpha} & \boldsymbol{K}_{\alpha\beta} \\ \boldsymbol{K}_{\beta\alpha} & \boldsymbol{K}_{\beta\beta} \end{bmatrix} \begin{bmatrix} \Delta\boldsymbol{\alpha} \\ \Delta\boldsymbol{\beta} \end{bmatrix} = \begin{bmatrix} \boldsymbol{R}_\alpha \\ \boldsymbol{R}_\beta \end{bmatrix}$
      with $\Delta\boldsymbol{\varphi} = 0, \Delta\boldsymbol{\chi} = 0, \Delta\boldsymbol{\tau}_\chi = 0, \Delta\boldsymbol{w}_\tau = 0$
    - ▶ update nodal values for the single element $\begin{aligned} \boldsymbol{\alpha}^{j,k+1} &= \boldsymbol{\alpha}^{j,k} + \Delta\boldsymbol{\alpha} \\ \boldsymbol{\beta}^{j,k+1} &= \boldsymbol{\beta}^{j,k} + \Delta\boldsymbol{\beta} \end{aligned}$
    - ▶ calculate local residuals $\boldsymbol{R}_L = \left\{ \boldsymbol{R}_\alpha \ \boldsymbol{R}_\beta \right\}^T$ and check if $\boxed{\| \boldsymbol{R}_L \|_\infty < TOL_L}$
  - **end**
  - ▶ calculate global residuals $\boldsymbol{R}_G = \left\{ \boldsymbol{R}_\varphi \ \boldsymbol{R}_\chi \ \boldsymbol{R}_\tau \ \boldsymbol{R}_w \right\}^T$
  - ▶ calculate all tangents and the related **consistent tangents** by setting $\boldsymbol{R}_\alpha = \boldsymbol{0}$ and $\boldsymbol{R}_\beta = \boldsymbol{0}$
  - ▶ solve system of equations

$$\begin{bmatrix} \boldsymbol{K}_{\varphi\varphi\text{cons}} & \boldsymbol{K}_{\varphi\chi\text{cons}} & \boldsymbol{K}_{\varphi\tau\text{cons}} & \boldsymbol{K}_{\varphi w\text{cons}} \\ \boldsymbol{K}_{\chi\varphi\text{cons}} & \boldsymbol{K}_{\chi\chi\text{cons}} & \boldsymbol{K}_{\chi\tau\text{cons}} & \boldsymbol{K}_{\chi w\text{cons}} \\ \boldsymbol{K}_{\tau\varphi\text{cons}} & \boldsymbol{K}_{\tau\chi\text{cons}} & \boldsymbol{K}_{\tau\tau\text{cons}} & \boldsymbol{K}_{\tau w\text{cons}} \\ \boldsymbol{K}_{w\varphi\text{cons}} & \boldsymbol{K}_{w\chi\text{cons}} & \boldsymbol{K}_{w\tau\text{cons}} & \boldsymbol{K}_{ww\text{cons}} \end{bmatrix} \begin{bmatrix} \Delta\boldsymbol{\varphi} \\ \Delta\boldsymbol{\chi} \\ \Delta\boldsymbol{\tau}_\chi \\ \Delta\boldsymbol{w}_\tau \end{bmatrix} = \begin{bmatrix} \boldsymbol{R}_\varphi \\ \boldsymbol{R}_\chi \\ \boldsymbol{R}_\tau \\ \boldsymbol{R}_w \end{bmatrix}$$

  - ▶ update nodal values $\begin{aligned} \boldsymbol{\varphi}^{j+1} &= \boldsymbol{\varphi}^j + \Delta\boldsymbol{\varphi} & \boldsymbol{\tau}_\chi^{j+1} &= \boldsymbol{\tau}_\chi^j + \Delta\boldsymbol{\tau}_\chi \\ \boldsymbol{\chi}^{j+1} &= \boldsymbol{\chi}^j + \Delta\boldsymbol{\chi} & \boldsymbol{w}_\tau^{j+1} &= \boldsymbol{w}_\tau^j + \Delta\boldsymbol{w}_\tau \end{aligned}$
  - ▶ calculate global residuals $\boldsymbol{R}_G = \left\{ \boldsymbol{R}_\varphi \ \boldsymbol{R}_\chi \ \boldsymbol{R}_\tau \ \boldsymbol{R}_w \right\}^T$ and check if $\boxed{\| \boldsymbol{R}_G \|_\infty < TOL_G}$
- **end**

end

Energy density formulation

$$\begin{aligned}\psi \quad &= \underbrace{c_1\left(\boldsymbol{I}:\boldsymbol{C}-3-2\log\left(J\right)\right)+\frac{\lambda}{2}\left(\left[\log\left(J\right)\right]^2+\left(J-1\right)^2\right)}_{\text{Neo-Hooke}}+c_3\boldsymbol{n}_0\cdot\boldsymbol{C}\boldsymbol{n}_0\\ &+c_3\left(\boldsymbol{I}:\left(\boldsymbol{n}_t\otimes\boldsymbol{n}_t\right)-1\right)+\underbrace{\left(c_9+a\right)\left|\boldsymbol{F}^T\boldsymbol{n}_t\right|^2+\left(c_{10}-a\right)\left(\boldsymbol{n}_0\cdot\boldsymbol{F}^T\boldsymbol{n}_t\right)^2}_{\text{[Biggins et al. (2008)]}}\\ &+\underbrace{\frac{c_{12}}{2}\left[\left(\boldsymbol{\alpha}-\boldsymbol{\beta}\right)\times\boldsymbol{n}_t\right]^2}_{\text{[Warner and Terentjev (2007), Concas and Groß (2024)]}}+c_{14b}\left[\left(\boldsymbol{\alpha}-\boldsymbol{\beta}\right)\cdot\boldsymbol{F}\boldsymbol{n}_0\right]^2\end{aligned}$$

Material parameters

[Anderson et al. (1999), de Luca et al. (2013)]

- $c_1=\dfrac{\mu}{2}$
- $c_3=\dfrac{\mu\left(r-1\right)}{2}$
- $c_9=\dfrac{\mu}{2}\left(\dfrac{1}{r}-1\right)$
- $c_{10}=\dfrac{\mu}{2}\left(2-\dfrac{1}{r}-r\right)$
- $a=0.063\,\dfrac{\mu}{2}$
- $c_{12}=0.25\,\mu$
- $c_{14b}=4\,\mu$
- $\lambda=\dfrac{2}{3}\mu\left(\dfrac{1+\nu}{1-2\nu}-1\right)$
- $r=\dfrac{\ell_{\parallel}}{\ell_{\perp}}$

Numerical test: LCE film under orientational surface load

Specimen geometry

virtual specimen with $H/L = 1$ ($12.5 \times 12.5 \times 0.3$ mm) and 900 $H1-$elements

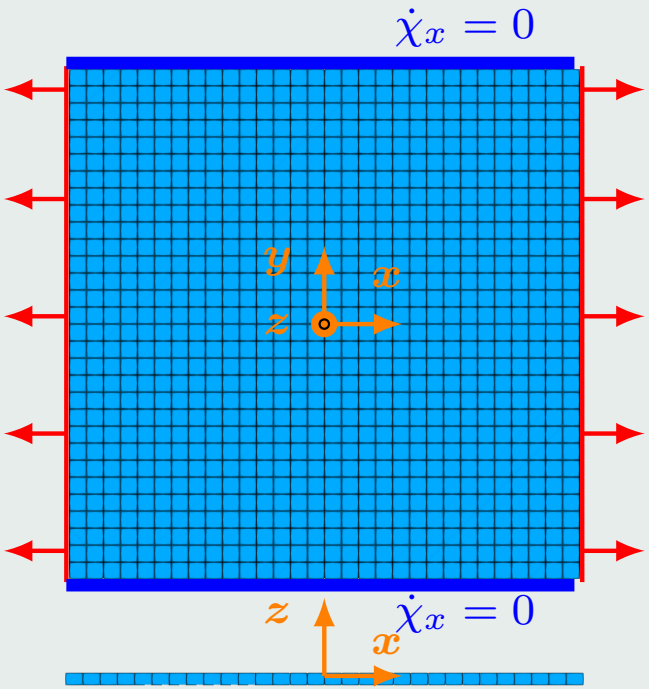

$$\boldsymbol{W} = 4.4\,\mu N/s$$
$$\boldsymbol{n}_0 = \boldsymbol{e}_y$$

- orientational surface load in the direction e_x on both vertical sides of the film
- orientational Dirichlet boundary condition ($\dot{\chi}_x = 0$) on the other two sides of the film

Parameters

[de Luca et al. (2013), Groß et al. (2022)]

- $cG(k = 2)$
- $h_n = 0.002\,s$
- $t_{end} = 0.04\,s$
- $TOL_G = 10^{-12}$ and $TOL_L = 10^{-14}$
- $\|\boldsymbol{R}_G\|_\infty < TOL_G$ and $\|\boldsymbol{R}_L\|_\infty < TOL_L$
- $E = 0.914\,MPa$
- $\nu = 0.493$
- $\rho = 1760\,kg/m^3$
- $r(T = 60°C) = 1.88$
- $V_\beta = 200\,Pa \cdot s$

Numerical test: LCE film under orientational surface load

- **with** orientational Dirichlet boundary condition at $t = 0.4\,s$

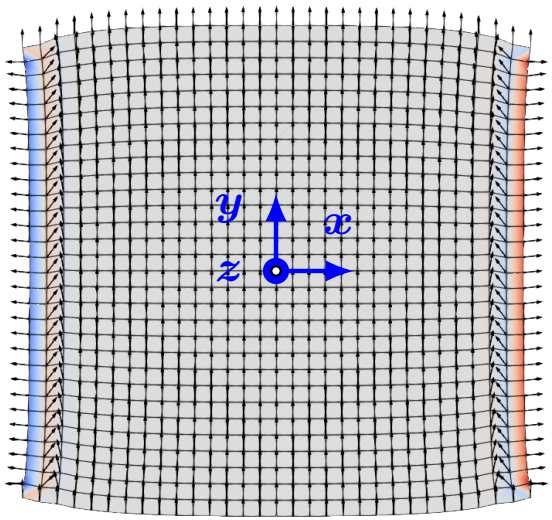

-8.771e+05 $\tau_{\chi\,x}\,[Pa]$ 8.771e+05

- **without** orientational Dirichlet boundary condition at $t = 0.4\,s$

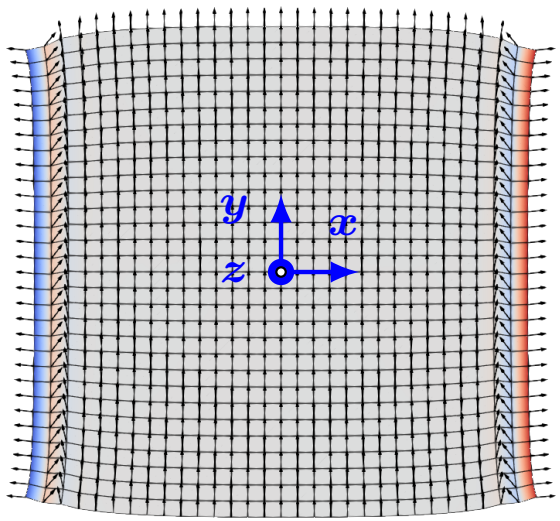

-6.667e+05 $\tau_{\chi\,x}\,[Pa]$ 6.667e+05

orientational Dirichlet boundary condition

- applied in the variational formulation by means of the reaction force $\boldsymbol{R}_{\chi}$ as Lagrange multiplier
- rotation of nematic directors about the $z-$direction for the nodes in the vertices is impeded even though they undergo the orientational surface load $\boldsymbol{W}$
- distribution of the $x-$component of the reorientation stress vector $\boldsymbol{\tau}_{\chi}$ shows that the central part of the virtual specimen is unaffected, with $\boldsymbol{\tau}_{\chi}$ as Lagrange multiplier for the constraint

$$\dot{\boldsymbol{\chi}} = \left(\dot{\boldsymbol{\alpha}} - \dot{\boldsymbol{\beta}}\right) \times \boldsymbol{\chi}$$

Numerical test: LCE film under orientational surface load

Error of the momentum balances and moment of momentumum balances

Balance laws

cf. principle of virtual power from Concas and Groß (2023), (2024)

$$\boldsymbol{L}\left(t_{n+1}\right)-\boldsymbol{L}\left(t_{n}\right)=\iint\limits_{\mathscr{T}_n\times\mathscr{B}_0}\rho_0\boldsymbol{B}_\varphi\,\mathrm{d}V\,\mathrm{d}t+\iint\limits_{\mathscr{T}_n\times\partial_T\mathscr{B}_0}\boldsymbol{T}\,\mathrm{d}A\,\mathrm{d}t+\iint\limits_{\mathscr{T}_n\times\partial_\varphi\mathscr{B}_0}\boldsymbol{R}\,\mathrm{d}A\,\mathrm{d}t$$

$$\boldsymbol{J}\left(t_{n+1}\right)-\boldsymbol{J}\left(t_{n}\right)=\iint\limits_{\mathscr{T}_n\times\mathscr{B}_0}[\boldsymbol{\varphi}\times\rho_0\boldsymbol{B}_\varphi]\,\mathrm{d}V\,\mathrm{d}t+\iint\limits_{\mathscr{T}_n\times\partial_T\mathscr{B}_0}[\boldsymbol{\varphi}\times\boldsymbol{T}]\,\mathrm{d}A\,\mathrm{d}t+\iint\limits_{\mathscr{T}_n\times\partial_\varphi\mathscr{B}_0}[\boldsymbol{\varphi}\times\boldsymbol{R}]\,\mathrm{d}A\,\mathrm{d}t$$
$$-\iint\limits_{\mathscr{T}_n\times\mathscr{B}_0}\left(\boldsymbol{F}\times\frac{\partial\psi}{\partial\boldsymbol{F}}\right)\mathrm{d}V\,\mathrm{d}t+\iint\limits_{\mathscr{T}_n\times\mathscr{B}_0}\left(\frac{\partial\psi}{\partial\boldsymbol{\alpha}}+\frac{\partial\psi}{\partial\boldsymbol{\beta}}\right)\mathrm{d}V\,\mathrm{d}t+\iint\limits_{\mathscr{T}_n\times\mathscr{B}_0}\boldsymbol{\Sigma}_\beta\,\mathrm{d}V\,\mathrm{d}t$$

- multi-level procedure

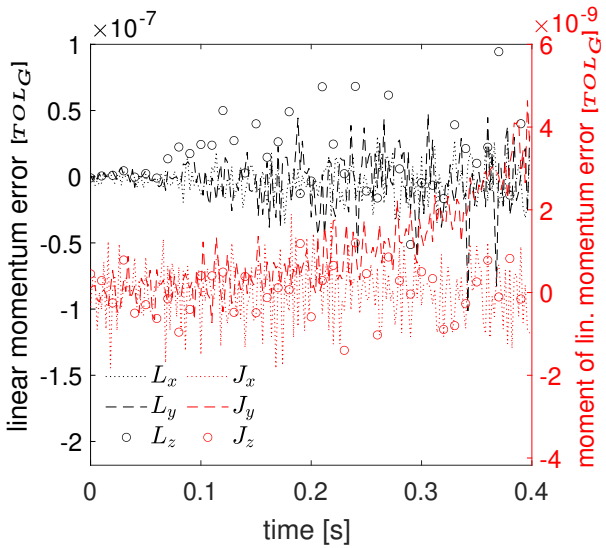

- global-level procedure

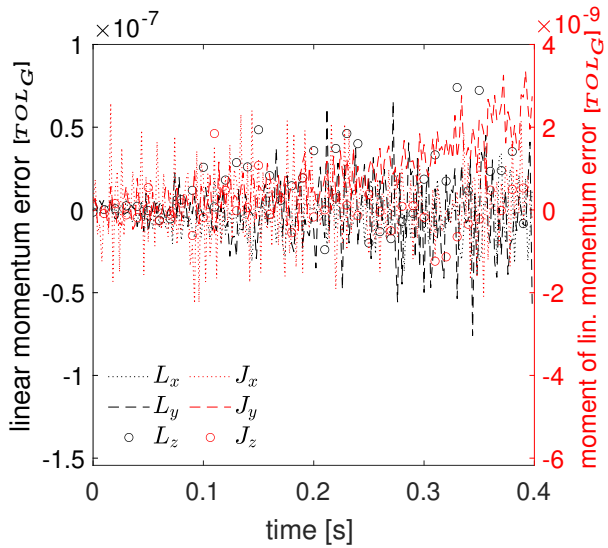

Numerical test: LCE film under orientational surface load

Error of the orientational momentum balances and moment of orientational momentum balances

Balance laws

cf. principle of virtual power from Concas and Groß (2023), (2024)

$$\boldsymbol{L}_\chi(t_{n+1}) - \boldsymbol{L}_\chi(t_n) = \iint_{\mathscr{T}_n \times \mathscr{B}_0} \left[\rho_0 \boldsymbol{B}_\chi - \boldsymbol{\tau}_\chi - \frac{\partial \psi}{\partial \boldsymbol{\chi}}\right] \mathrm{d}V\,\mathrm{d}t + \iint_{\mathscr{T}_n \times \partial_W \mathscr{B}_0} \boldsymbol{W}\,\mathrm{d}A\,\mathrm{d}t + \iint_{\mathscr{T}_n \times \partial_\chi \mathscr{B}_0} \boldsymbol{R}_\chi\,\mathrm{d}A\,\mathrm{d}t$$

$$\boldsymbol{J}_\chi(t_{n+1}) - \boldsymbol{J}_\chi(t_n) = \iint_{\mathscr{T}_n \times \mathscr{B}_0} [\boldsymbol{\chi} \times \rho_0 \boldsymbol{B}_\chi]\,\mathrm{d}V\,\mathrm{d}t + \iint_{\mathscr{T}_n \times \partial_W \mathscr{B}_0} [\boldsymbol{\chi} \times \boldsymbol{W}]\,\mathrm{d}A\,\mathrm{d}t + \iint_{\mathscr{T}_n \times \partial_\chi \mathscr{B}_0} [\boldsymbol{\chi} \times \boldsymbol{R}_\chi]\,\mathrm{d}A\,\mathrm{d}t - \iint_{\mathscr{T}_n \times \mathscr{B}_0} \left[\boldsymbol{\chi} \times \left(\boldsymbol{\tau}_\chi + \frac{\partial \psi}{\partial \boldsymbol{\chi}}\right)\right] \mathrm{d}V\,\mathrm{d}t$$

- multi-level procedure

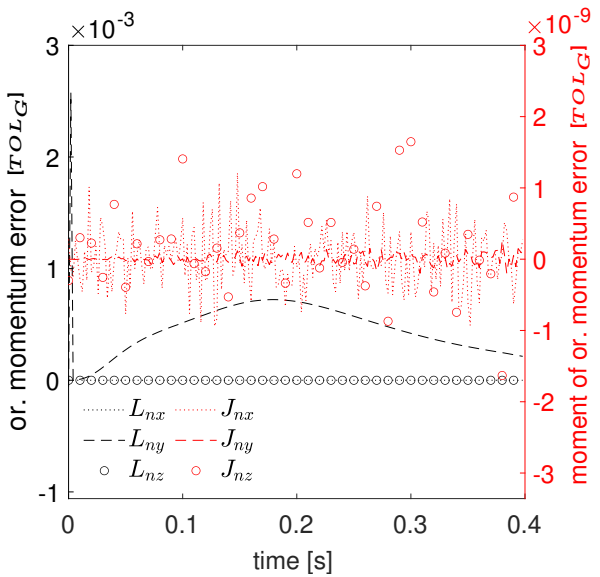

- global-level procedure

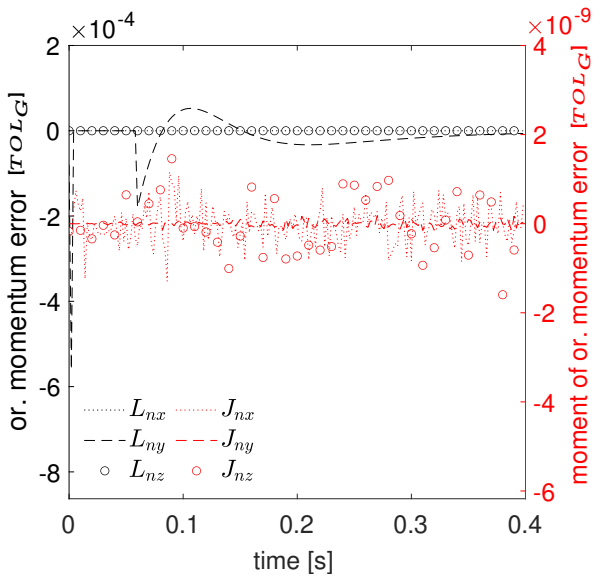

Numerical test: LCE film under orientational surface load

Trends of global and local residuals

- multi-level procedure
  - trend of global residual vs number of iterations

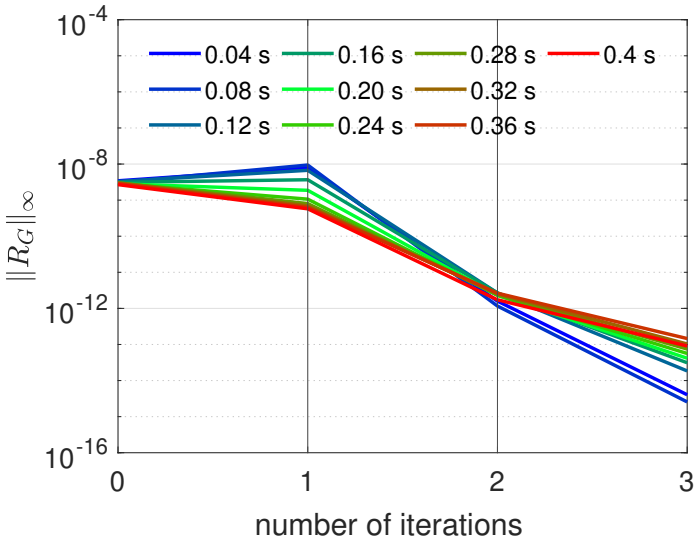

  - sum of local residual over elements vs time

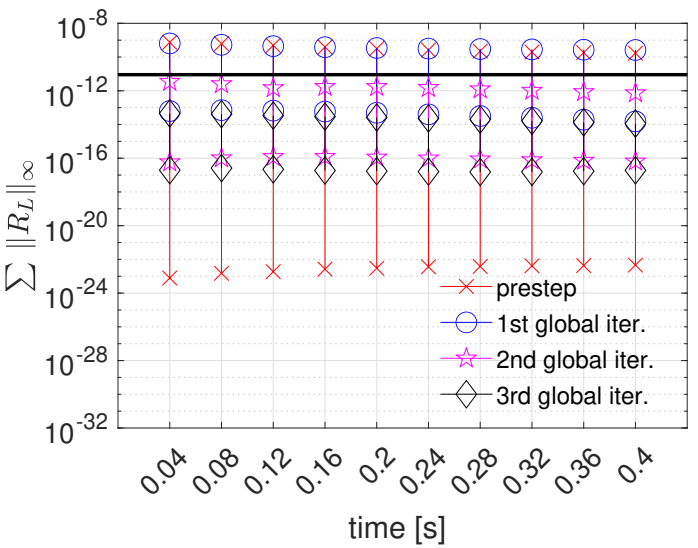

- global-level procedure
  - trend of global residual vs number of iterations

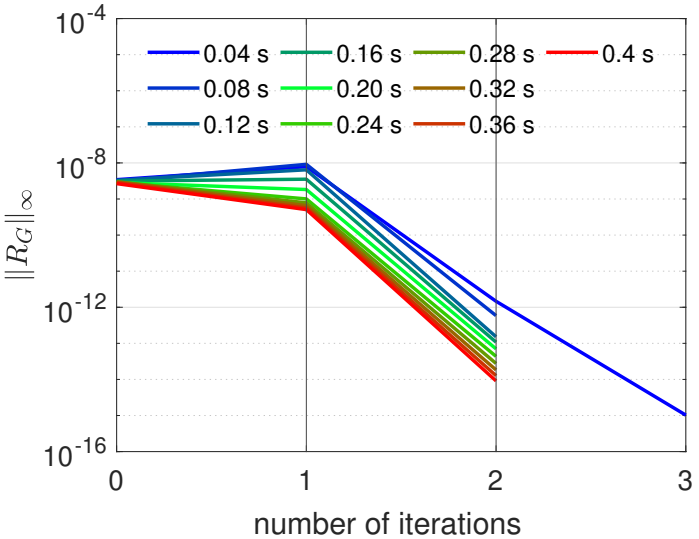

Global residual $\boldsymbol{R}_G$ and local residual $\boldsymbol{R}_L$

$$\boldsymbol{R}_G = \left\{ \begin{array}{c} \boldsymbol{R}_\varphi \\ \boldsymbol{R}_\chi \\ \boldsymbol{R}_\tau \\ \boldsymbol{R}_w \end{array} \right\} \quad \text{and} \quad \boldsymbol{R}_L = \left\{ \begin{array}{c} \boldsymbol{R}_\alpha \\ \boldsymbol{R}_\beta \end{array} \right\}$$

- trends of residuals for 20 of overall 200 time steps
- values of the previous time step for $\boldsymbol{\varphi}$, $\boldsymbol{\chi}$, $\boldsymbol{\tau}_\chi$, $\boldsymbol{w}_\tau$, $\boldsymbol{\alpha}$ and $\boldsymbol{\beta}$ are used as initial guess for the current time step ($j = 0$ or $k = 0$)
- global residual $\boldsymbol{R}_G$ fulfills the convergence criterion after three iterations ($j = 3$) for all time steps by using the multi-level procedure
- local residual $\boldsymbol{R}_L$ fulfills the convergence criterion after only one iteration ($k = 1$) for all time steps

Numerical test: LCE stripe under orientational volume load

Specimen geometry

virtual specimen with $H/L = 40$ ($28 \times 1120 \times 84\ \mu$m) and 480 $H1-$elements

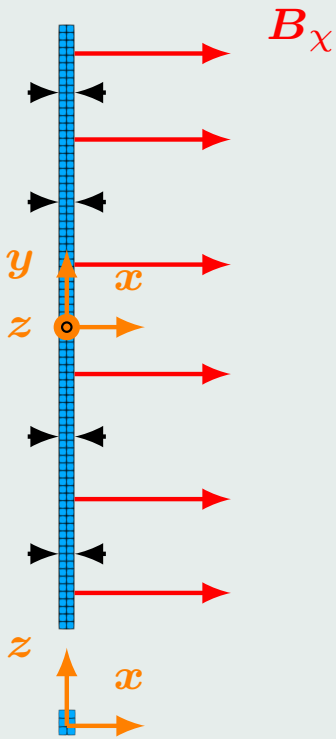

$$B_\chi = 500\, m^2/s^2$$
$$n_0 = e_y$$
$$\dot{\varphi}_x = 0$$

- linearly increasing volume load over time up to ($500\,\mathrm{m}^2/\mathrm{s}^2$) in the direction e_x
- virtual experiment similar to the one described by Urayama et al. (2006) for swollen nematic elastomer under electric field
- deformational Dirichlet boundary condition ($\dot{\varphi}_x = 0$) on both vertical sides of the stripe
- compressible material and 20-times lower rotational viscosity V_β in order to achieve full rotation of the mesogens

Parameters

[de Luca et al. (2013), Groß et al. (2022)]

- $cG(k=2)$
- $h_n = 0.002\, s$
- $t_{end} = 0.04\, s$
- $TOL_G = 10^{-12}$ and $TOL_L = 10^{-14}$
- $\|\boldsymbol{R}_G\|_\infty < TOL_G$ and $\|\boldsymbol{R}_L\|_\infty < TOL_L$
- $E = 0.914\, MPa$
- $\nu = 0.3$
- $\rho = 1760\, kg/m^3$
- $r(T = 60°C) = 1.88$
- $V_\beta = 10\, Pa \cdot s$

Numerical test: LCE stripe under orientational volume load

- virtual specimen at $t = 0\ s$
- specimen at $t = 0.4\ s$ (**multi-level**)
- specimen at $t = 0.4\ s$ (**global-level**)

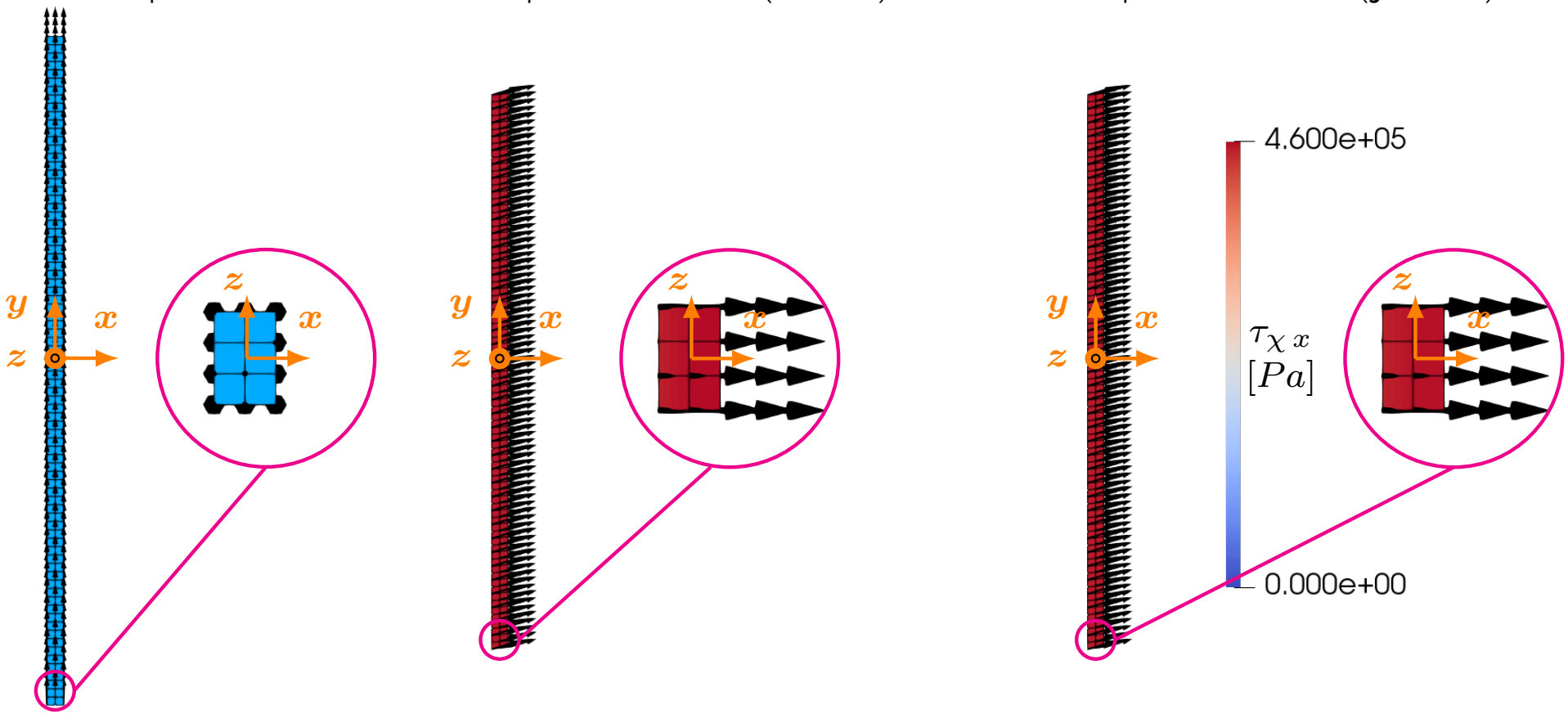

Results

- full rotation of the mesogens leads to contraction in the $y-$direction and slight extension in the $z-$direction of the virtual specimen
- no noticeable difference in the distribution of the reorientation stress vector $\boldsymbol{\tau}_\chi$ ($x-$component) resulting from the two different procedures

Numerical test: LCE stripe under orientational volume load

Trends of global and local residuals

- multi-level procedure
  - trend of global residual vs number of iterations

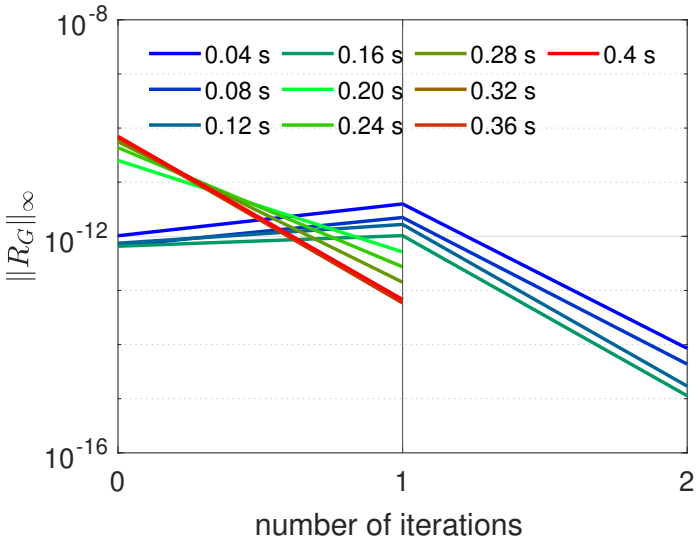

  - sum of local residual over elements vs time

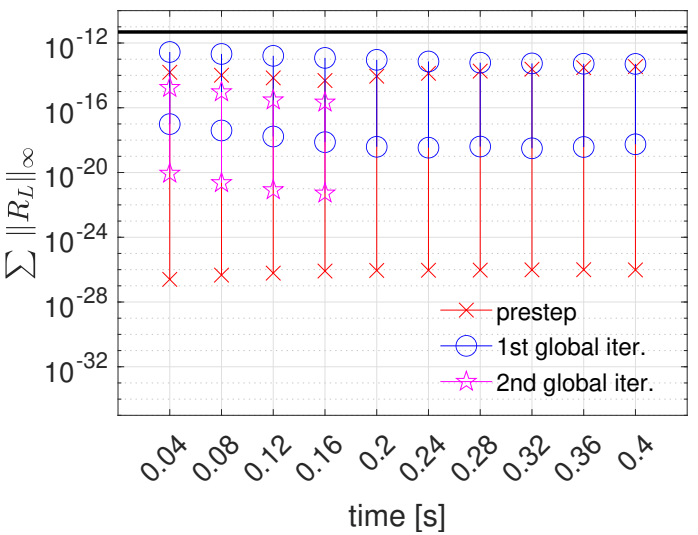

- global-level procedure
  - trend of global residual vs number of iterations

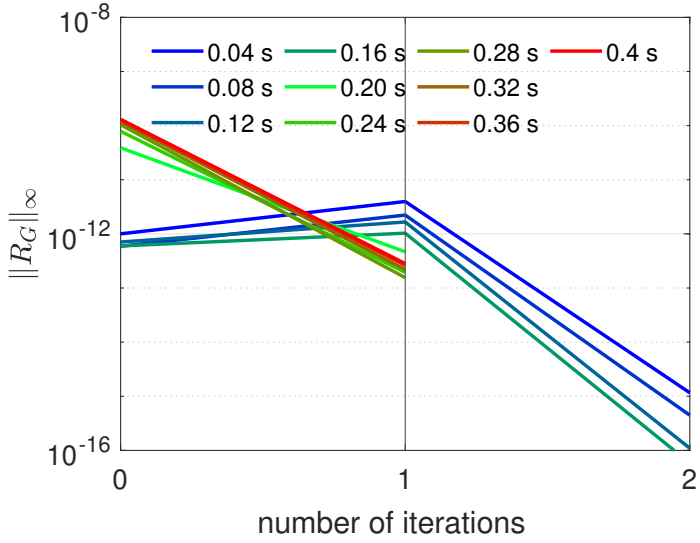

Global residual $\boldsymbol{R}_G$ and local residual $\boldsymbol{R}_L$

$$\boldsymbol{R}_G = \left\{ \begin{array}{c} \boldsymbol{R}_\varphi \\ \boldsymbol{R}_\chi \\ \boldsymbol{R}_\tau \\ \boldsymbol{R}_w \end{array} \right\} \quad \text{and} \quad \boldsymbol{R}_L = \left\{ \begin{array}{c} \boldsymbol{R}_\alpha \\ \boldsymbol{R}_\beta \end{array} \right\}$$

- trends of residuals for 20 of overall 200 time steps
- values of the previous time step for $\boldsymbol{\varphi}$, $\boldsymbol{\chi}$, $\boldsymbol{\tau}_\chi$, $\boldsymbol{w}_\tau$, $\boldsymbol{\alpha}$ and $\boldsymbol{\beta}$ are used as initial guess for the current time step ($j = 0$ or $k = 0$)
- global residual $\boldsymbol{R}_G$ fulfills the convergence criterion after only one iteration ($j = 1$) from $t = 0.164\ s$
- local residual $\boldsymbol{R}_L$ fulfills the convergence criterion after only one iteration ($k = 1$) for all time steps

Computation time

- multi-level procedure (**volume load with 480 H1-elements**)

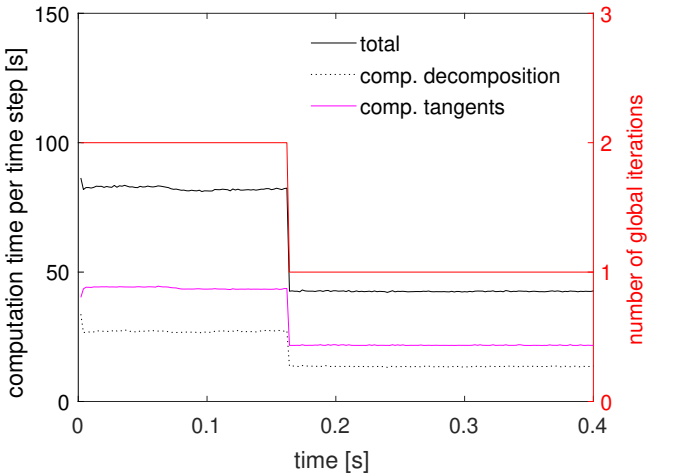

- global-level procedure (**volume load with 480 H1-elements**)

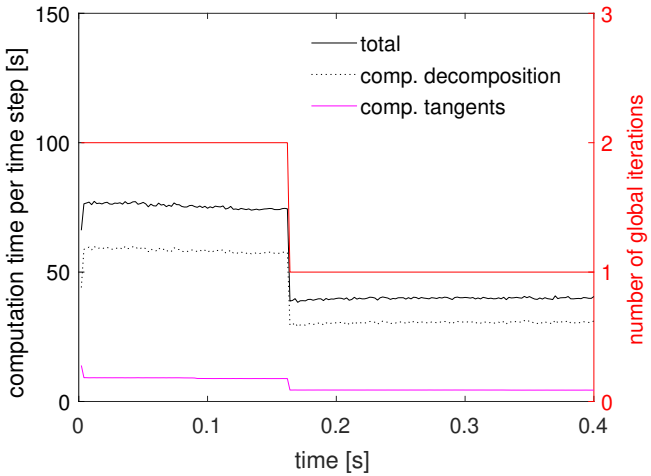

- multi-level procedure (**surface load with 900 H1-elements**)

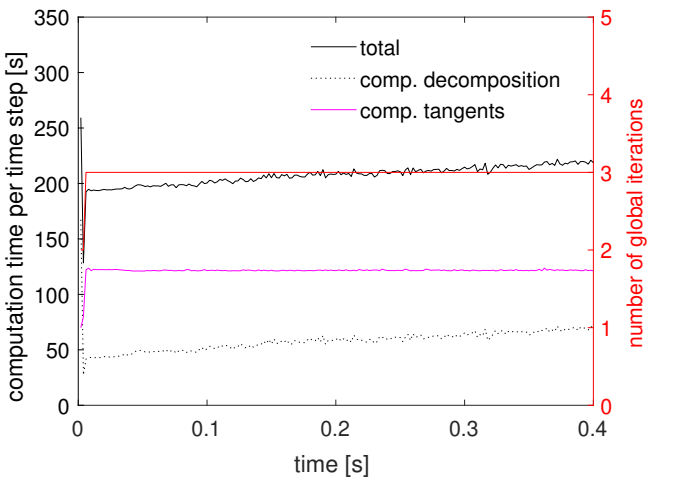

- global-level procedure (**surface load with 900 H1-elements**)

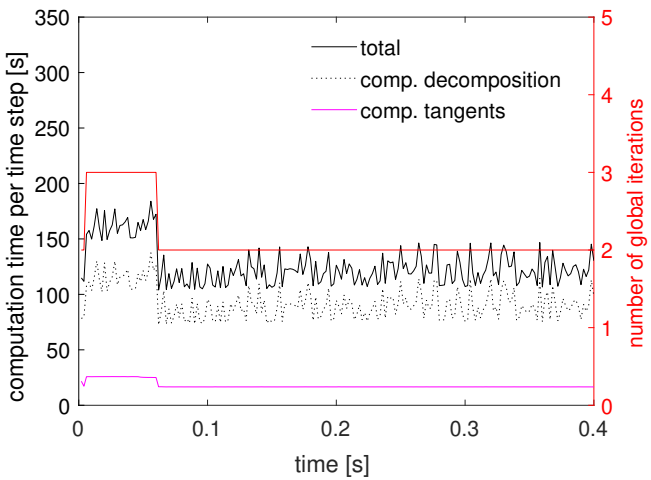

Main tasks influencing the computation time

- decomposition, i.e. LU-factorization of the global tangent (prevailing by global-level procedure)
- calculation of consistent tangents (prevailing by multi-level procedure)

Conclusion

- multi-level procedure has been implemented for reducing the dimension of the global system of equations
- simulation results given by the multi-level procedure are analogous to those given by the global-level procedure
- including the new rotational free energy density $\psi_{14b} = c_{14b} \left[(\boldsymbol{\alpha} - \boldsymbol{\beta}) \cdot \boldsymbol{F}\boldsymbol{n}_0 \right]^2$ makes tangents at the *element*-level non-singular
- numerical algorithm conserves all mechanical balances
- in some cases, multi-level procedure may require more global iterations, which contributes to increase the total computation time

Future work

- use different degrees of approximations at the *element*-level in **space** and **time** in order to improve convergence of the multi-level procedure
- parallelize LU-factorization and calculation of tangents
- parallelization for LU-factorization is more challenging than parallelization for tangent calculation, as additional hardware and software are needed (cf. Bartelt et al. (2020), Sabir and Alebrahim (2025))